Direct Imaging of the InSb(001)-$c(8 \times 2)$ Surface: Evidence for Large Anisotropy of the Reconstruction

T. D. Mishima,[2] N. Naruse,[1,2,*] S. P. Cho,[2] T. Kadohira,[2] and T. Osaka[1,2]

[1]*Department of Materials Science and Engineering, Waseda University, Shinjuku-ku, Tokyo 169-0072, Japan*

[2]*Kagami Memorial Laboratory for Materials Science and Technology, Waseda University, Nishiwaseda, Shinjuku-ku, Tokyo 169-0051, Japan*

(Received 23 April 2002; published 20 December 2002)

We have observed the InSb(001)-$c(8 \times 2)$ surface by using high-resolution transmission electron microscopy in the profile-imaging geometry. All images observed at temperatures up to 420 °C agree well with the $c(8 \times 2)$ model reported by Kumpf *et al.* [Phys. Rev. Lett. **86**, 3586 (2001)]. 1/30 sec real-time observations at 420 °C evidence that a part of the subsurface and surface layers (called a gull-type segment) undergo switching to and from a bulk configuration. The finding is suggestive of large anisotropy in the mean square displacement of the $c(8 \times 2)$ surface.

DOI: 10.1103/PhysRevLett.89.276105 PACS numbers: 68.35.Bs, 68.35.Ja, 68.37.Lp

All the (001) surfaces of III-V compound semiconductors exhibit a wealth of reconstructions, depending on V/III element ratios and substrate temperature. The reconstructed structure which emerges commonly to most of these surfaces under group-III-element stabilized conditions has a (4×2) and/or a $c(8 \times 2)$ unit [1–6]. It has been accepted so far that the $c(8 \times 2)$ unit mesh is formed by staggering the rows of two (4×2) subunits in the [110] direction by $\times 1$ [5,7]. Although atomic arrangements of the (4×2) and $c(8 \times 2)$ units are believed to be essentially identical, there has been considerable debate over where and to what extent group III dimers are present in their unit cell [8–12].

This problem seems to reach a clear solution by the most recent clarification for details of the respective atomic structures: Lee *et al.* proposed on the basis of density-functional-theory calculations and low energy electron diffraction measurements that the GaAs(001)-$c(8 \times 2)$ surface is reconstructed with the so-called $\zeta(4 \times 2)$ structural unit, preserving Ga dimers in the second and the third layer [13]. Paget *et al.* strongly supported the $\zeta(4 \times 2)$ model using x-ray diffraction (XRD) analyses and first-principles total energy calculations [14]. Kumpf *et al.* also refer to group III dimers with 100% occupancy in the third layer and with a reduced occupancy in the second layer of $c(8 \times 2)$ surfaces by XRD using direct methods [15]. Here, we draw attention to the structural model for the InSb(001)-$c(8 \times 2)$ surface proposed by Kumpf *et al.,* especially focusing on the existing state of In dimer. Real-space observations associated with the $c(8 \times 2)$ surface, even though limited to InSb, have been energetically carried out so far by scanning tunneling microscopy (STM) [1,3,7]. However, STM experiments have not captured yet dimers having a certain occupancy in the second layer and also those at a larger depth of the third layer.

In this Letter, we present the direct imaging of InSb(001)-$c(8 \times 2)$ surface and its dynamical structural changes by using high-resolution transmission electron microscopy in the profile-imaging geometry (HR-profile TEM). This Letter describes for the first time direct observation of (i) dimers in the third layer, (ii) a reduced occupancy of In atom in the second layer, and (iii) that a part of the $c(8 \times 2)$ surface layers, specifically In dimers in the third layer and their on-top region (a part of the first and second layers), changes into the bulk lattice and is instantaneously back to the original surface, without desorbing Sb even at 420 °C.

A detailed description of the UHV *in situ* HR-TEM used in this study has been given in our previous papers [16,17]. InSb single crystals (nondoped) were crushed with an agate mortar and pestle under purified ethanol. The resulting fragmentary specimens, each of which included some low index surfaces such as (001), (110), and (111), were then mounted onto a holey carbon microgrid. In the TEM specimen chamber, the native oxide was removed from the surfaces by heating the specimens at 460 °C with impinging Sb_4 molecules. Immediately after cleaning, several scores Å of InSb were grown homoepitaxially on the surfaces at 300 °C with In_1 (2.8×10^{14} atoms cm^{-2} min^{-1}) and Sb_4 (1.4×10^{15} atoms cm^{-2} min^{-1}) molecular beams. The surfaces were annealed for several hours at a temperature of 420 °C that a single phase of $c(8 \times 2)$ emerges on {001} types of surfaces [2]. HR-profile TEM images were recorded with a very small specimen beam current density of ~ 1 $A\,cm^{-2}$ on a video cassette recorder. Multislice simulations for the images were performed using the commercial MACTEMPAS program.

Figure 1 shows a low magnification TEM image taken while observing a specimen piece of InSb at a temperature of 300 °C that stably keeps the $c(8 \times 2)$ surface of lnSb(001). The TEM image gives us two pieces of crystallographic information that serve for identifying an InSb(001) surface: One is the InSb(111)A-(2×2) surface with a well-known vacancy buckling structure [18],

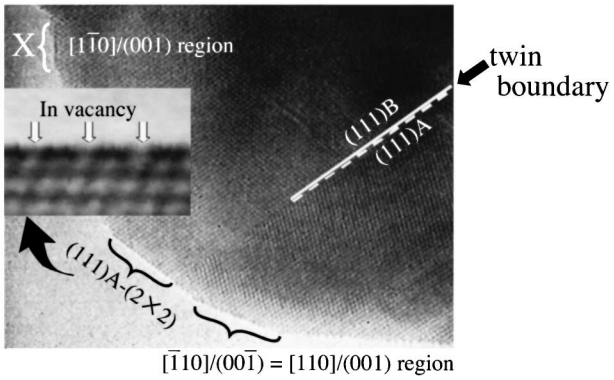

FIG. 1. A low magnification TEM image taken while observing a specimen piece of InSb at 300 °C. We can see the (001) surface from both azimuths of [110] and [1$\bar{1}$0], because the [110] direction on the (001) surface is equivalent to [$\bar{1}$10] on (00$\bar{1}$). The inset is an HR-profile image of the (111)*A*-(2 × 2) surface.

which enables us to observe the (001) surface viewed from the [1$\bar{1}$0] azimuth. The other is a twin boundary existing accidentally in the observed area. On the basis of these, we can specify the [110]/(001) region equivalent to the [$\bar{1}$10] on the (00$\bar{1}$).

Figures 2(a) and 2(b) show a part of through-focal series HR-profile TEM images taken at 300 °C from the [110]/(001) and the [1$\bar{1}$0]/(001) region in Fig. 1, respectively. These images output from S-VHS videotapes in an averaging mode (four frames were averaged) were adopted to construct a possible structure model for the

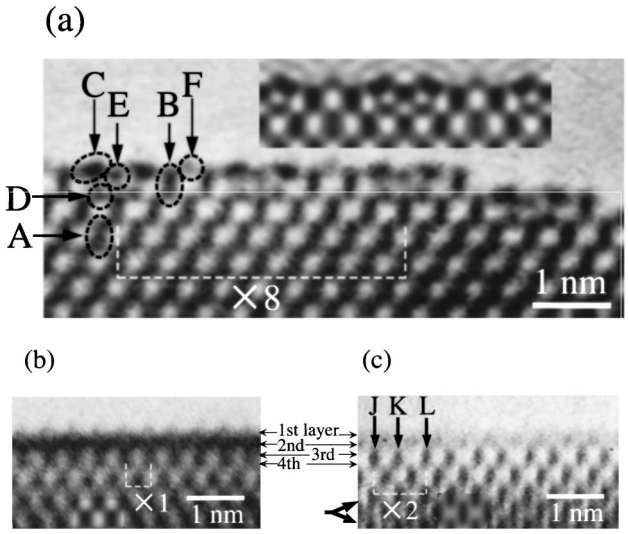

FIG. 2. HR-profile TEM images for the InSb(001)-*c*(8 × 2) surface taken from [110] (a), and [1$\bar{1}$0] direction (b), (c). From the defocus values of (a) −48 nm, (b) −29 nm, and (c) −58 nm, the respective crystal thicknesses are estimated to be 4.0 nm for (a), 5.5 nm for (b), and 2.0–3.0 nm for (c). The insets in (a)–(c) are the images simulated at each defocus, especially, (a) is the simulated image of the structural model proposed by Kumpf *et al.*

c(8 × 2) surface through an evaluation of crystal thickness. The bulk part of Fig. 2(a) taken under the nearly Scherzer-focused condition agreed well with the image simulated at a crystal thickness of 4.0 nm. This thickness was confirmed also by the simulations for the vacancy buckling structure of the InSb(111)*A*-(2 × 2) surface near the [110]/(001) region in Fig. 2(a). Thus, we judged the outermost part of the image to be regarded as so-called structure image in this crystal thickness, in which the individual spots exhibiting dark contrast reflect surface atomic rows. Figure 2(a) clearly shows up a ×4 periodicity at the outermost surface. Further, we can find elongated dark spots in the bulk part of this figure, representatively marked with *A*, to correspond to the atomic rows of In-Sb. Atomic rows that belong to the remaining dark spots in Fig. 2(a), *B*–*F* were assigned by adopting the *A* spot as a standard and by carrying out the line-profile analysis: The line profile obtained from the *B* and *C* spots was almost similar to that from *A*. Comparing with *A*, the *D* and *E* spots are smaller in size and weaker in contrast, each being estimated to be around 60% ~ 70% occupancy within accuracy of the line-profile analysis. The occupancy of the *F* spot that has further low contrast was a half extent of that of *A*. A structure model for the [110] projection, derived from the assignments of *A* to *F*, is shown in Fig. 3(a).

Next, it is very interesting to compare the [110]-projection model of Fig. 3(a) with Figs. 2(b) and 2(c) taken along the [1$\bar{1}$0] azimuth. In Fig. 2(b), obscure protrusions in the outermost surface are seen with ×1 periodicity and are most likely to correspond to the first layer in Fig. 3(a). However, the second layer underneath it has been embedded in the bandlike contrast. Since, if the bandlike contrast is brought by a superimposition of atomic rows, the thickness of the specimen used, 5.5 nm is too thick to resolve the above atomic rows, another HR-profile TEM image [Fig. 2(c)] was taken at 300 °C along the [1$\bar{1}$0] projection of a thinner specimen. The resulting TEM image makes it possible to light up the individual atomic rows hiding in the bandlike contrast region. Contrasts of the In-Sb bilayers indicated by a branched arrow in Fig. 2(c) matched exceedingly well with the [1$\bar{1}$0] simulations at a crystal thickness of 3.0 nm. Judging from a decrease of the photographic density from the bilayer region toward the outermost layer, this specimen is most likely wedge shaped, yielding an averaged thickness of about 2.0 nm in the region between the first and the fourth layer. Further, the following information was gained from Fig. 2(c): Distances between *J* and *K* and between *K* and *L* are seen to be evidently different and are estimated to be ~0.4 nm for the *J*-*K* distance and ~0.5 nm for *K*-*L*, measured by using the interval between In-Sb pairs in Fig. 2(c) as a standard. This means that in the [110] atomic row perpendicular to the [1$\bar{1}$0] there exist two types of bond lengths, the shorter one suggesting the presence of dimer. As is well known, the reconstructed (001) surface of semiconductors such as Si

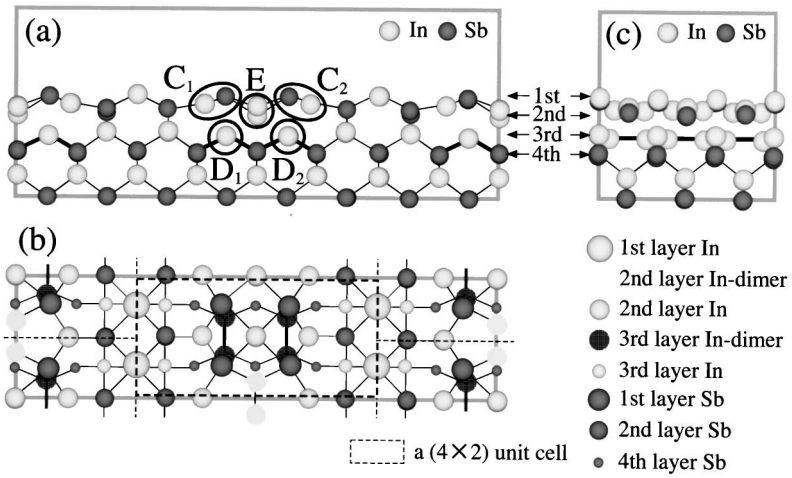

FIG. 3. Schematic illustration of a structural model for the InSb(001)-$c(8 \times 2)$ surface: (a) side view from [110], (b) top view, and (c) side view from $[1\bar{1}0]$.

and GaAs often has a dimer in its fundamental structure. According to the most recent paper related with the InSb(001)-$c(8 \times 2)$ surface, reported by Kumpf *et al.* [15], the subsurface (the second and third layers) comprises In-In dimers in itself. However, the -0.4 nm interval in our measurements is much larger than a dimer length of 0.272–0.289 nm reported by previous works [8,15] and is sufficiently large even when compared with 0.324 nm which is the smallest separation of atoms in the body-centered tetragonal lattice of bulk In.

We explored the origin of this interval by examining the contrast of an atomic row aligned parallel to the [110] direction in the bilayer corresponding to the third and fourth layers, represented by J in Fig. 2(c). The $\sim$2.0 nm thickness of J corresponds closely to one (4×2) block in the $c(8 \times 2)$ surface region (for one block 1.83 nm in $[1\bar{1}0]$). The third layer having this thickness is most likely to include two In dimers. In order to assess whether these dimers have effects on atomic rows below the fourth layer, first, we performed multislice simulations for the (4×2) subunit in the Kumpf *et al.* model. However, the simulated images finally reproduced well the J-K and K-L intervals, only when the fourth–sixth layers are displaced by $\sim$0.02–0.05 nm from each bulk position. Figures 3(b) and 3(c) show possible structure models for the top view and the $[1\bar{1}0]$ projection, which were depicted on the basis of Fig. 3(a) and the above examination, respectively. These figures are almost all consistent with the structure model proposed by Kumpf *et al.*, except that In dimers (D spot) in the third layer and In atoms (E spot) in the second layer have reduced site occupancies of around 70% and around 60%, respectively. Main disagreement between the direct image taken at 300 °C [Fig. 2(a)] and the images simulated on the basis of the Kumpf *et al.* model [inserted into Fig. 2(a)] is due to differences in In dimer occupancy in the third layer and in In atom occupancy in E of the second layer. This is also confirmed from the fact that, as mentioned in the foregoing paragraph, the D and E spots in Fig. 2(a), which reflect In dimer rows, evidently have weaker contrast than bulk column. [110]-projection images simulated for the other $c(8 \times 2)$ models reported in the previous works [8,9,12,19,20] fundamentally did not agree well with Fig. 2(a), except for the ζ model extremely similar to the Kumpf *et al.* model.

A further straightforward step associated with In dimers in the third layer is to make it clear whether or not the reduced site occupancy is dependent on temperature. Figures 4(a)–4(f) show a series of profile-TEM images taken at 420 °C from the $c(8 \times 2)$ surface near the region observed in Fig. 2(a), during an extremely short duration of 19/30 sec. An S-VHS video recorder used allows 1/30 sec real-time observations at 420 °C. The 1/30 frame observation led us to unpredicted structural changes taking place at the narrow region put between the first and the third layer and indicated by two white arrows in Figs. 4(a)–4(f). This region (hereafter,

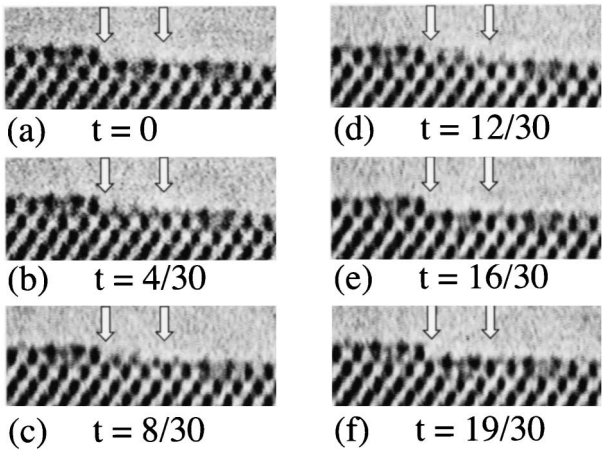

FIG. 4. A real-time sequence of HR-profile TEM images showing dynamical structural changes in the $c(8 \times 2)$ surface.

called a "gull-type" segment) undergoes switching to and from a bulk configuration as follows: The head and legs parts [E and D, respectively, in Fig. 3(a)] of the gull-type segment transformed into the stronger contrast comparable to In-Sb pair in bulk and simultaneously its wings part (C_1, C_2) altered its contrast into the weaker one, as can be seen in Figs. 4(a) and 4(b). It follows that the wings part seems to be place exchanged by the head and legs parts, leaving three atomic rows in the outermost layer. However, during dynamical processes toward Fig. 4(d), two of the three atomic rows changed to appear bulklike, though they exhibited somewhat low contrast as compared with that of an In-Sb bulk pair. More surprisingly, after 7/30 sec from Fig. 4(d), the collapsed gull-type segment returned to the original reconstructed surface. The reason why the remaining atomic row leaves solely can be explained as follows: The total number of atoms associated with the above-mentioned place exchange is balanced only when In atoms and In dimers have around 60% and 70% occupancies in E of the second layer and in the third layer, respectively. Such structural changes demonstrate that at 420 °C the $c(8 \times 2)$ surface is allowed to change reversibly from the gull-type segment to bulk lattice without any change in surface stoichiometry.

This reversible structural change gives us very important information about the Debye-Waller (DW) factors for the $c(8 \times 2)$ reconstructed surface. According to Kumpf *et al.*, although all atoms constituting the gull-type segment have larger DW values than those of bulk, they are isotropic. Further, the most recent report related with GaAs-$c(8 \times 2)$ [21] refers to in-plain anisotropy in the DW factor for Ga atoms forming an atomic row corresponding to E in Fig. 3(a). However, no work that presents the anisotropy evidence on DW factors for the $c(8 \times 2)$ surface based on the direct observation has been carried out so far. Figures 4(a)–4(f) are the first evidence that, of atoms existing on the $c(8 \times 2)$ surface, the atoms constituting the gull-type segment have considerably large anisotropy in their DW factors.

Finally, care must be taken for the experimental results obtained above. It is required to test effects of electron beam irradiation on the surface processes. As mentioned in the experimental paragraph, a series of the profile-TEM images was taken under a small beam current of $\sim 1\ A\,cm^{-2}$ at 420 °C as well as other temperatures. This beam current is likely to be too sufficiently small to induce such dynamical structural changes on the $c(8 \times 2)$ surface, because even under irradiation by a highly concentrated beam of $100\ A\,cm^{-2}$ used by Iijima *et al.* [22] the temperature of small particle specimens is not higher than 100 °C, and therefore the beam current density of $\sim 1\ A\,cm^{-2}$ at most brings the increase in a temperature of a few degrees of celsius.

In conclusion, we have presented the direct imaging of the InSb(001)-$c(8 \times 2)$ surface by using HR-profile TEM. Every image taken at temperatures up to 420 °C evidenced the existence of In atoms and In dimers with a reduced site occupancy in the outermost and second layers and in the third layer, respectively. The results were confirmed by multislice simulations and also agreed well with those reported by Kumpf *et al.* Furthermore, the real-time observations at 420 °C for the first time displayed that, once the gull-type segment of the $c(8 \times 2)$ surface was altered into the bull lattice, it was instantaneously restored to the original reconstruction. This suggests that the whole constituent atoms of the gull-type segment may have large anisotropy in their DW factors.

We would like to thank Dr. A. Ohtake, Dr. M. Nishizawa, and Dr. J. Nakamura for their valuable discussion and critical comments, and also G. Sakoda and M. Hagimoto for their technical support. This work was partially supported by a Grant-in-Aid for Scientific Research (B) (Grant No. 12450299) from the Ministry of Education, Science, Sports and Culture, by a Waseda University Grant for Special Research Projects (No. 2001A-554), by a Grant for the promotion of the advancement of education and research in graduate schools, and by a Grant-in-Aid for Research for the Future from the Japan Society for the Promotion of Science.

*Corresponding author.
Email address: naruse@asagi.waseda.jp

[1] For example, Q. -K. Xue, T. Hashizume, and T. Sakurai, *Scanning Tunneling Microscopy of III-V Compound Semiconductor (001) Surfaces*, in Advances in Scanning Probe Microscopy, edited by T. Sakurai and Y. Watanabe (Springer-Verlag, Berlin, 2000).
[2] W. K. Liu and M. B. Santos, Surf. Sci. **319**, 172 (1994).
[3] C. F. McConville *et al.*, Phys. Rev. B **50**, 14 965 (1994).
[4] C. Kendrick, G. Lelay, and A. Kahn, Phys. Rev. B **54**, 17 877 (1996).
[5] J. Cerdà, F. J. Palomares, and F. Soria, Phys. Rev. Lett. **75**, 665 (1995).
[6] P. De Padova *et al.*, Surf. Sci. **482–485**, 587 (2001).
[7] A. A. Davis *et al.*, Appl. Phys. Lett. **75**, 1938 (1999).
[8] P. John *et al.*, Phys. Rev. B **39**, 1730 (1989).
[9] S. L. Skala *et al.*, Phys. Rev. B **48**, 9138 (1993).
[10] M. O. Schweitzer *et al.*, Surf. Sci. **280**, 63 (1993).
[11] P. R. Varekamp *et al.*, Surf. Sci. **350**, L221 (1996).
[12] N. Jones *et al.*, Surf. Sci. **409**, 27 (1998).
[13] S. H. Lee, W. Moritz, and M. Scheffler, Phys. Rev. Lett. **85**, 3890 (2000).
[14] D. Paget *et al.*, Phys. Rev. B **64**, 161305(R) (2001).
[15] C. Kumpf *et al.*, Phys. Rev. Lett. **86**, 3586 (2001); C. Kumpf *et al.*, Phys. Rev. B **64**, 75307 (2001).
[16] T. Mishima and T. Osaka, Surf. Sci. **395**, L256 (1998).
[17] T. Mishima *et al.*, J. Vac. Sci. Technol. B **16**, 2324 (1998).
[18] J. Bohr *et al.*, Phys. Rev. Lett. **54**, 1275 (1985).
[19] D. K. Biegelsen *et al.*, Phys. Rev. B **41**, 5701 (1990).
[20] S. Ohkouchi and N. Ikoma, Jpn. J. Appl. Phys., Pt. 1 **33**, 3770 (1994).
[21] A. Ohtake *et al.*, Phys. Rev. B **65**, 233311 (2002).
[22] S. Iijima and T. Ichihashi, Phys. Rev. Lett. **56**, 616 (1986).